THE JOURNAL OF BIOLOGICAL CHEMISTRY
Vol. 274, No. 6, Issue of February 5, pp. 3503–3512, 1999
Printed in U.S.A.

The Structure of the Site on Adenovirus Early Region 1A Responsible for Binding to TATA-binding Protein Determined by NMR Spectroscopy*

(Received for publication, June 4, 1998, and in revised form, September 26, 1998)

David P. Molloy‡, K. John Smith§, Anne E. Milner‡, Phillip H. Gallimore‡¶, and Roger J. A. Grand‡‖

From the ‡CRC Institute for Cancer Studies, University of Birmingham, Edgbaston, Birmingham B15 2TA, United Kingdom and §School of Biochemistry, University of Birmingham, Edgbaston, Birmingham B15 2TT, United Kingdom

Previous detailed mutational analysis has shown that the binding site on adenovirus (Ad) early region 1A (E1A) for TATA-binding protein (TBP) is located toward the N terminus of conserved region 3 (CR3). Here we demonstrate that synthetic peptides of between 15 and 22 amino acids, identical to amino acid sequences of CR3 present in the larger Ad5 E1A (13 S product) and in both the Ad12 E1A (13 and 12 S products) proteins that lie N-terminal to the zinc finger motif, can disrupt binding of E1A to TBP. These findings suggest that the peptides are biologically active in terms of interacting with TBP and must therefore comprise some, if not all, of the TBP binding site on E1A. The interaction between Ad12 E1A and TBP was confirmed by direct co-precipitation experiments. In ^{1}H NMR studies of CR3 peptides, regular patterns of NOEs were observed from which their conformational preferences in aqueous solution were determined. Both Ad5 and Ad12 peptides were shown to contain regions of helical backbone structure in 50% trifluoroethanol. In each case, the type and intensities of NOE cross-peaks observed correlated best to α-helical turns. These helices are more extensive in larger peptides and extend from Glu^{141} to Val^{147} and from Arg^{144} to Pro^{152} in the full-length Ad5 and Ad12 13S E1A proteins, respectively. The structure of a 19-residue Ad5 CR3 peptide carrying the V147L mutation in the full-length protein that abolishes TBP binding was examined. No significant differences between the substituted and wild type peptides were observed, suggesting that this substitution in the intact protein may cause disruption of global rather than local structures.

Adenovirus early region 1A (E1A)[1] encodes two major proteins (of sedimentation coefficients 13 and 12 S and of 289 and 243 amino acids, respectively, in Ad5), which are identical except for the presence of an additional "unique" region toward the C terminus of the larger molecule. Either together or separately, they are capable of inducing a variety of effects in mammalian cells. Following viral infection, they stimulate expression of other viral genes (1, 2) and can enhance or repress expression of cellular genes (3, 4). In addition, introduction of E1A DNA into cells can have profound biological effects. For example, it can induce apoptosis, primarily through increasing p53 expression (5, 6), induce DNA synthesis and cell cycle progression in quiescent cells (7, 8), inhibit differentiation (9, 10), and under certain circumstances induce morphological transformation (11). It seems likely that all of these results are attributable to the ability of the E1A proteins to interact with and modify the activity of important cellular regulators (reviewed in, for example, Refs. 12 and 13).

Although E1A proteins from different virus serotypes have many properties in common, certain important differences have been noted. Most significantly, group A adenoviruses (*e.g.* Ad12) can cause tumors in newborn rodents, while the group C viruses (*e.g.* Ad2 and Ad5) are nononcogenic. These differences have been attributed to activities of E1A (reviewed in Ref. 14). However, comparison of the amino acid sequences of E1As from different virus serotypes has indicated a number of highly conserved regions (CR). Mutational and biochemical analysis has demonstrated that these are involved in many although not all of the interactions with cellular proteins. For example, E1A binds to the retinoblastoma gene product pRb and related proteins p107 and p130 through conserved region 1 (amino acids 40–80) and conserved region 2 (amino acids 120–139; Refs. 15 and 16). Additionally, interaction of E1A with the transcriptional regulator p300 is through CR1 and the much less well conserved N-terminal domain (17, 18). A further complex formed by E1A involves a short region very close to the C terminus, which although not identified as a conserved region in the original studies (19, 20) is highly homologous in proteins from different viral serotypes. This domain of E1A is involved in interaction with a 48-kDa cellular phosphoprotein termed the C-terminal binding protein (21).

Of central importance to the role of Ad E1A as a regulator of gene expression is the "unique" conserved region 3, which is only present in its entirety in the larger E1A component. The C terminus of the domain binds certain members of the ATF family of DNA binding proteins (22–25). In addition, the CR3 region is probably involved in interaction with the cellular YY1 transcription factor (26). However, the best characterized protein-protein interaction involving conserved region 3 is with the TATA-binding protein (TBP), the DNA binding subunit of transcription factor IID (27, 28). The binding site involves the zinc finger domain of CR3 (29–31) and the adjacent amino acid sequence N-terminal to this (28, 32). Sequences located toward the N terminus of the protein have also been implicated in the interaction (33).

The contribution of each amino acid in Ad5 CR3 to TBP

* This work was supported by the Cancer Research Campaign. The costs of publication of this article were defrayed in part by the payment of page charges. This article must therefore be hereby marked "*advertisement*" in accordance with 18 U.S.C. Section 1734 solely to indicate this fact.

¶ A Cancer Research Campaign Gibbs Fellow.

‖ To whom correspondence should be addressed: CRC Institute for Cancer Studies, University of Birmingham, Edgbaston, Birmingham B15 2TA, United Kingdom. Tel.: 0121-414-4471; Fax: 0121-414-4486; E-mail: R.J.A.Grand@bham.ac.uk.

[1] The abbreviations used are: E1A, early region 1A; CR, conserved region; Ad, adenovirus; TBP, TATA-binding protein; GST, glutathione S-transferase; aa, amino acid(s); TOCSY, total correlation spectroscopy; NOESY, nuclear Overhauser effect spectroscopy.

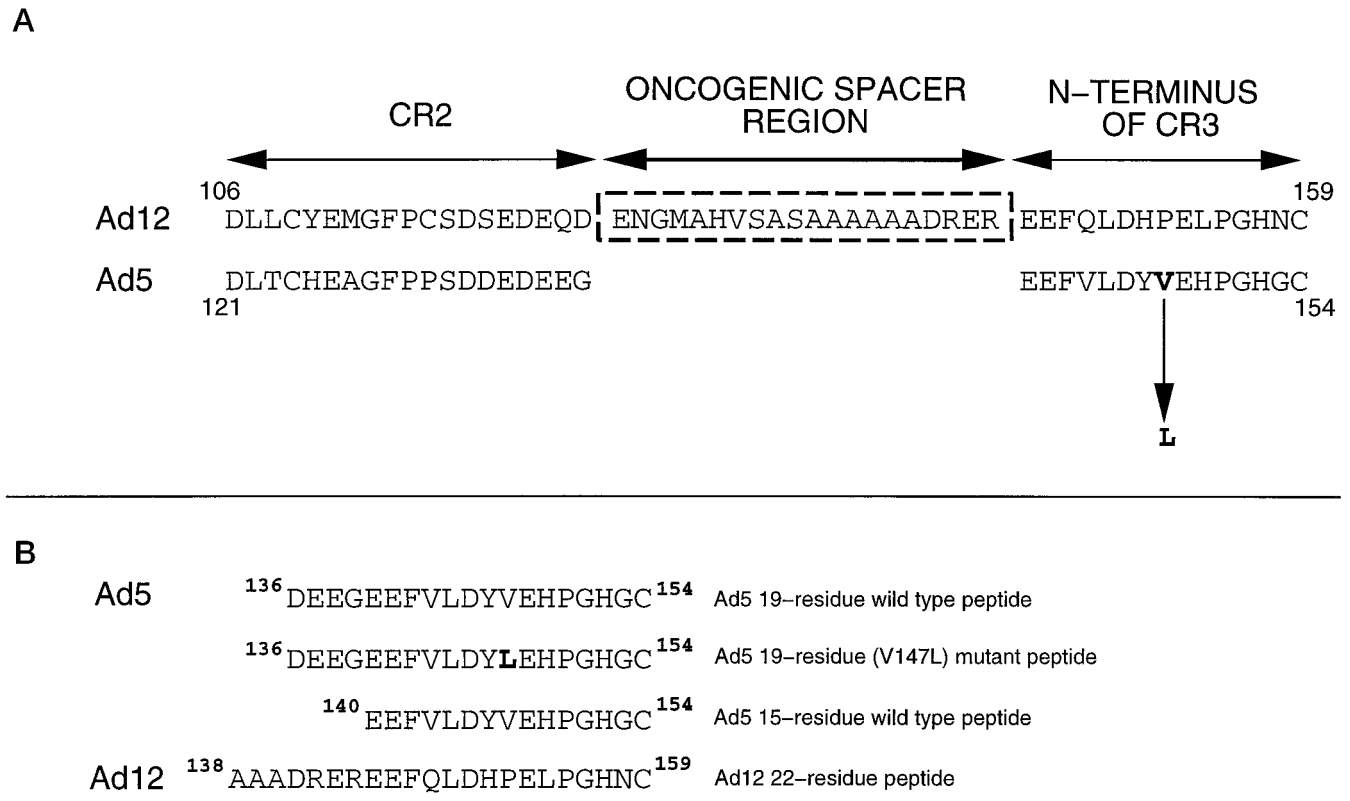

FIG. 1. **Amino acid sequences of Ad5 and Ad12 13 S E1A proteins and peptides.** *A*, the sequences of Ad5 (residues 121–154) and Ad12 (residues 106–159) 13 S E1A are shown. While CR2 and CR3 are adjacent in Ad5, these regions are separated in Ad12 by the 20-aa oncogenic spacer region. The *arrow below* the Ad5 sequence shows the biologically significant substitution V147L that disrupts E1A binding to TBP (32). *B*, the amino acid sequences of the four synthetic peptides used in this study.

binding and to trans-activation has been studied in detail (28, 30, 32). However, it is not clear whether the zinc finger forms part of the interface or is simply required for the overall three-dimensional structure of the region (discussed in Ref. 34). While mutation of cysteine residues in CR3 (the zinc-coordinating amino acids) leads to a marked reduction in TBP binding (32), it has been shown that point mutations in the region N-terminal to the zinc finger also inhibit the interaction with TBP. In addition, the substitutions V147L, E148G, P150A, and G151A on Ad5 E1A or deletion of amino acids 139–149 reduced binding to TBP (28, 32).

In the work described here, we set out to analyze whether that portion of Ad E1A CR3, N-terminal to the zinc finger domain, was capable of interaction with TBP. In addition, the three-dimensional structure of the region was examined. These studies have been carried out using short synthetic peptides equivalent to the N-terminal sequences of Ad5 and Ad12 CR3 (Fig. 1). It has long been known that small synthetic peptides corresponding to sequences from proteins can adopt secondary structures analogous to that seen in the intact molecule. Such peptides are most frequently found to adopt either helical (35), or β-turn (36, 37) secondary structures, since the key interactions required to maintain the conformation (including hydrogen bonds) are short range and limited only by the number of amino acids within the peptide. Where a synthetic peptide mimics the structure of a binding site within a protein, it is clearly possible for that peptide also to mimic complex biological functions associated with the protein. For example, it has been shown that a peptide equivalent to CR3, when microinjected into cells, will activate expression from the adenovirus major late promoter (38).

In the study presented here, we have shown that peptides equivalent to sequences from CR3 in both Ad5 and Ad12 E1A can inhibit binding of TBP to E1A. We have determined the structures of several peptides in solution by ^{1}H NMR spectroscopy and suggest that the helical conformation adopted by each of these peptides is similar to the TBP binding motif on CR3 in intact E1A.

EXPERIMENTAL PROCEDURES

Peptides—Four synthetic peptides identical in sequence to portions of conserved region 3 from both Ad5 13 S E1A and Ad12 13 S E1A were used in this study (Fig. 1). The peptides were synthesized by standard Fmoc (*N*-(9-fluorenyl)methoxycarbonyl) procedures (Alta Bioscience, University of Birmingham) and purified by high performance liquid chromatography on a Vydac C_{18} column eluted with a gradient of acetonitrile (0–60%) containing 0.1% trifluoroacetic acid.

Expression of Ad12 13 S E1A and Ad12 12 S E1A Proteins—The expression and purification of Ad12 E1A was performed as described (39). Ad12 13 S E1A and Ad12 12 S E1A were expressed in *Escherichia coli* strain TG2 using the pKK 388–1 expression vector. Three hours after induction of a 3.0-liter culture in the presence of 0.5 mM isopropyl-1-thio-β-D-galactopyranoside bacteria were harvested by centrifugation. E1A was then purified using essentially the protocol described earlier (39, 40). Pure E1A was renatured by prolonged dialysis against 10 mM NH_4HCO_3, pH 7.9, 1.5 mM β-mercaptoethanol at 4 °C (39). E1A was considered to have adopted a native conformation based on its ability to bind to TBP (see below), C-terminal binding protein, Rb p105, and zinc (39).

Expression of GST-TBP—TBP was expressed from a pGex vector in *Escherichia coli* strain TG2 as a fusion protein with glutathione S-transferase (GST; a generous gift from Dr. N. Jones, Imperial Cancer Research Fund, London, UK). GST-TBP was eluted from glutathione-agarose (Sigma) in the presence of 25 mM glutathione, and purity was determined by SDS-polyacrylamide gel electrophoresis.

Determination of Ad E1A-TBP Interactions by Western Blotting—Purified Ad12 E1A (15 μg in 10 μl of NETN buffer (50 mM Tris·HCl, pH 8.0, 100 mM NaCl, 1 mM EDTA, 0.5% Nonidet P-40)) was incubated with GST-TBP (60 μg in 30 μl of NETN buffer) at 4 °C. After 1 h, glutathione-agarose beads (50 μl) that had been preblocked with 5% skimmed milk powder were added. This mixture was agitated for 90 min at 4 °C. Agarose beads were retrieved by centrifugation and washed three times with NETN buffer. 5 mM glutathione (15 μl) was added to the washed

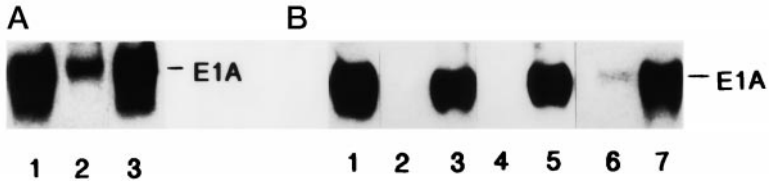

FIG. 2. **Western blot analysis of Ad12 12 S E1A and Ad12 13 S E1A complexes with GST-TBP.** *A*, binding of Ad12 12 S E1A and Ad12 13 S E1A to GST-TBP. GST-TBP was mixed with Ad12 E1A, and complexes were precipitated with glutathione-agarose beads. The bound E1A was determined by Western blotting (see "Experimental Procedures"). *Lane 1*, detection of Ad12 13 S E1A after elution from GST-TBP-glutathione-agarose beads; *lane 2*, detection of Ad12 12 S E1A after elution from GST-TBP-glutathione-agarose beads; *lane 3*, Ad12 13 S E1A standard. *B*, effect of E1A CR3 synthetic peptides on the interaction of E1A with GST-TBP. GST-TBP was mixed with peptide prior to incubation with E1A. E1A·GST-TBP complexes were precipitated on glutathione-agarose beads, and the amount of bound E1A was determined by Western blotting (see "Experimental Procedures"). *Lane 1*, Ad12 13 S E1A bound to GST-TBP as in *A*; *lanes 2* and *3*, E1A bound to GST-TBP after incubation in the presence of 12 nmol (*lane 2*) and 3 nmol (*lane 3*) of the 22-aa Ad12 CR3 peptide; *lanes 4* and *5*, E1A bound to GST-TBP after incubation in the presence of 12 nmol (*lane 4*) and 3 nmol (*lane 5*) of the 19-aa wild type Ad5 CR3 peptide; *lanes 6* and *7*, E1A bound to GST-TBP after incubation in the presence of 12 nmol (*lane 6*) and 3 nmol (*lane 7*) of the 19-aa mutant (V147L) Ad5 CR3 peptide.

agarose beads, and the released proteins were mixed with SDS-polyacrylamide gel electrophoresis sample buffer. After polyacrylamide gel electrophoresis and Western blotting, Ad12 E1A was detected using a mouse monoclonal antibody 5D02, developed by us.[2] The effect of synthetic Ad CR3 peptide on the Ad12 E1A-TBP interaction was monitored by incubating peptide with GST-TBP for 1 h prior to the addition of E1A.

Determination of Ad E1A-TBP Interactions by Enzyme-linked Immunosorbent Assay—The equilibrium dissociation constant (K_d) for Ad E1A CR3 peptides binding to GST-TBP was assessed by competition with purified bacterially expressed Ad12 266-aa E1A using an enzyme-linked immunosorbent assay technique essentially as described (37). Ninety-six-well plates were coated with Ad12 E1A (0.1 μg/well) by incubation overnight at 4 °C. E1A peptides serially diluted from 0 to 250 μg/ml were mixed with GST-TBP (10 μg/ml) for 30 min at 23 °C prior to adding to each well. After incubation for 1 h at 37 °C, the plates were washed six times with 0.1% Tween 80 in phosphate-buffered saline. TBP bound to E1A in the presence of synthetic peptide was determined on the plates with a goat antibody against GST followed by a horseradish peroxidase-linked antibody against goat IgG. Absorbance at 405 nm was measured after the addition of substrate using a Bio-Tek plate reader. Determinations were carried out in triplicate, and data were analyzed using a nonlinear least-squares approach (37).

CD Spectroscopy—Circular dichroism measurements were performed on an Applied Biophysics CD spectrometer using a 1-cm path length quartz cell at 25, 35, 45, 55, and 65 °C. Each spectrum was the average of five scans of peptide dissolved in 1 mM Tris·HCl, pH 7.4. Buffer background was subtracted. The concentrations of the wild type and V147L forms of the 19-aa Ad5 CR3 peptide were 100 μM.

NMR Spectroscopy—One-dimensional ^{1}H NMR data were collected on a Bruker AMX500 spectrometer using samples of peptide at 300 μM concentration in 25 mM [^{2}H]Tris, 5 mM [^{2}H]dithiothreitol adjusted to pH 7.4 with [^{2}H]Cl. A gated presaturation pulse of 1.5 s was used for accumulation over a 5000-Hz sweep width at an ambient probe temperature of 293 K with a 90° pulse of 5 μs. Spectra were recorded as 256 free induction decays and Fourier-transformed. GST-TBP and GST proteins used in one-dimensional experiments were dialyzed exhaustively against 25 mM [^{2}H]Tris, 5 mM [^{2}H]dithiothreitol adjusted to pH 7.4 with [^{2}H]Cl and added directly to the NMR tube to give ratios of peptide to protein of between 200:1 and 20:1. The pH was monitored directly in the NMR tube using an Ingold 3060 electrode and adjusted to pH 7.4 using [^{2}H]Cl or NaO[^{2}H].

Two-dimensional experiments were acquired using either a Bruker AMX500 spectrometer or a Varian Unity Plus 600-MHz spectrometer with 2048 data points in F2 with a sweep width of 11 ppm and with between 360 and 608 rows in F1. Solutions of peptide were between 5 and 10 mM in concentration, 285 K at pH 5.5 in 50% (v/v) trifluoroethanol (TFE)-d_3, 40% H_2O, 10% ^2H_2O. [^{2}H]Dithiothreitol was added to all peptide samples used in NMR spectroscopy to final concentrations of between 5 and 10 mM to prevent intermolecular disulfide bridge formation. The water resonance was suppressed by very weak presaturation applied during the relaxation delay (1.5 s) or by using a WATERGATE sequence (41). Solvent artifacts were suppressed using pulsed field gradients (42). Total correlation spectroscopy (TOCSY) used an MLEV-17 mixing pulse of 60-ms duration (10-kHz spin locking field). Nuclear Overhauser effect spectroscopy (NOESY) experiments were performed using mixing times of 100-, 200-, and 400-ms duration. Between 32 and 96 transients were acquired for TOCSY and double quantum-filtered correlation spectroscopy (COSY) experiments and between 96 and 128 transients for NOESY experiments. Assignments of proton signals in the peptides were based upon TOCSY and quantum-filtered correlation spectroscopy experiments to identify spin systems within individual residues that were then coupled to sequential NOE cross-peaks (*e.g.* $d_{\alpha N}(i, i + 1)$ in NOESY experiments. For the assignment of proline residues within the peptides, the δ-CH_2 proton signals were used in place of $d_{\alpha N}$ signals.

Interproton distances were estimated from NOESY experiments (200-ms mixing time duration) by integrating the contours for each cross-peak. The distances were then grouped into five classes between strong and very weak (the strong and medium NOEs were allocated the same distance constraints in structural calculations). The patterns of backbone hydrogen bonding within the peptides were assessed by following the movement of chemical shift of backbone amide protons with changes in temperature (at 285, 290, 295, 300, and 305 K) in TOCSY experiments. Temperature shift coefficients were calculated from the slope of a plot of temperature against chemical shift and were linear in every case.

The structures of peptides were determined using X-PLOR 3.8.5.1 (43) using a protocol in which certain atoms of each residue were embedded using the distance geometry routine (atoms CA, HA, N, HN, CB*, CG*, *dg_sub_embed* protocol). The remaining atoms were placed by template fitting, and then the atomic coordinates were allowed to evolve under the applied NOE distance constraints during a series of simulated annealing steps (*dgsa* and *refine* protocols). From the 100 structures generated, approximately 25–30 were discarded (wrong orientation in the distance geometry routine). The remaining structures were chosen with no violations of the applied NOEs of greater than 0.5 Å.

TFE was used as a co-solvent with water in this study, since it is well known that TFE/water mixtures enhance the solution structures of small peptides, primarily by providing an environment in which hydrogen bond formation within the peptide is promoted. TFE also reduces the formation of spurious secondary structures as a result of hydrophobic aggregation (44, 45).

RESULTS

It has previously been shown that the integrity of the N-terminal portion of Ad5 CR3 (aa 139–149) is essential for interaction of E1A with TBP and trans-activation (28, 32). However, there is little or no structural information available on E1A, and therefore the precise consequences of these deletions and mutations are unknown. Here, we have assessed whether synthetic peptides, identical in sequence to the N terminus of CR3 of Ad5 and Ad12 E1A (Fig. 1) interact with TBP. We have also examined the structure of the N-terminal portion of CR3, which comprises some, and perhaps all, of the TBP binding site on adenovirus E1A.

Binding of Ad12 E1A by TBP—Our initial aim was to demonstrate an interaction between TBP and E1A and then use this as an assay to determine the affinity of TBP for Ad E1A CR3 synthetic peptides. The Western blot presented in Fig. 2*A*

[2] P. H. Gallimore and R. J. A. Grand, unpublished data.

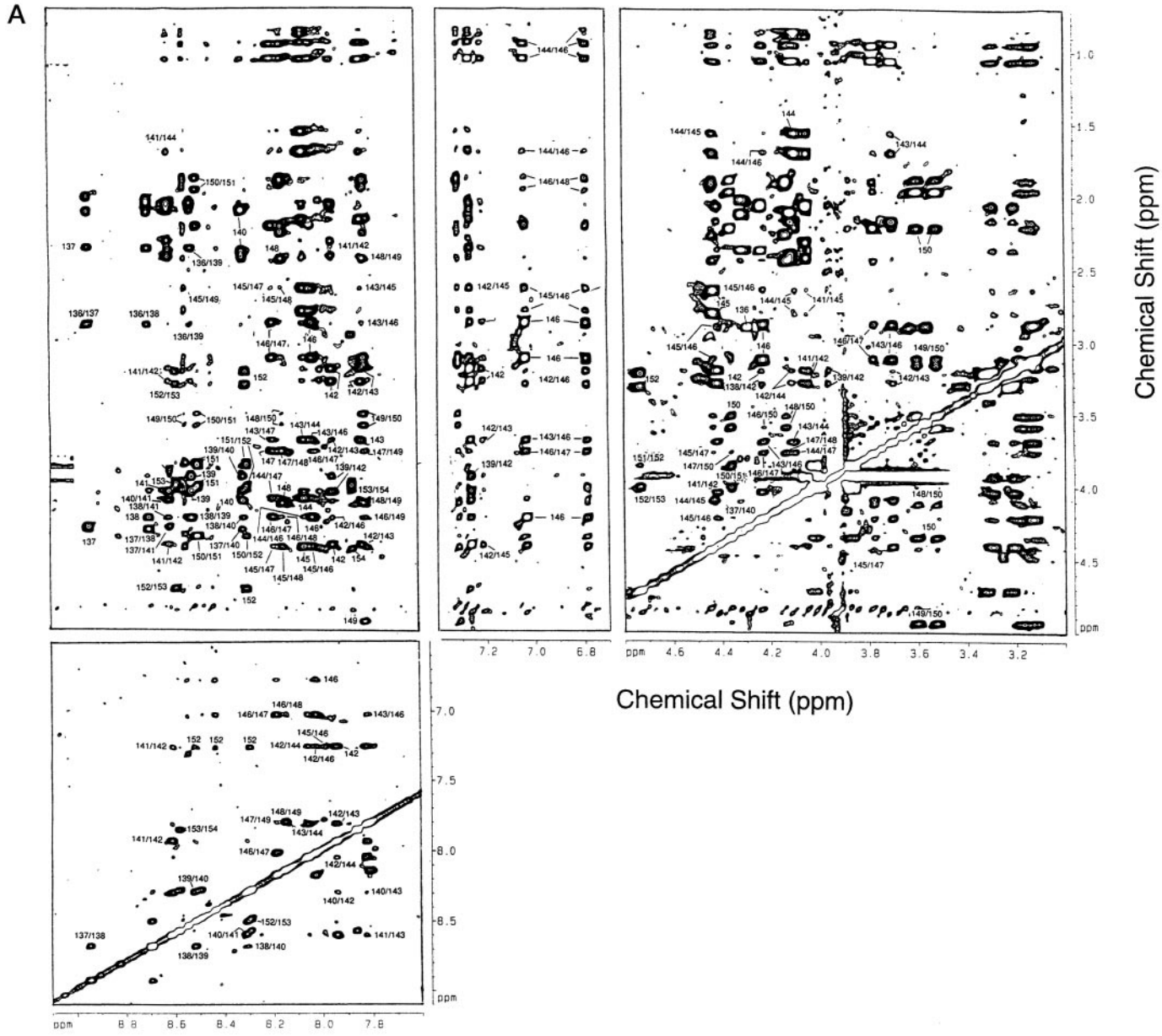

FIG. 3. **^{1}H NMR assignments and structural properties of the 19-aa wild type Ad5 (aa 136–154) peptide.** *A*, sections from a NOESY spectrum (200-ms mixing time) collected on a 10 mg/ml sample of the 19-residue wild type Ad5 CR3 peptide of sequence DEEGEEFVLDYVEHGHGC in 50% (v/v) TFE-d_3, 40% H_2O, 10% ^2H_2O, pH 5.5, at 285 K are presented. Cross-peaks within a single residue are labeled with a single number. Interresidue NOEs of the type $d_{NN}(i, i + 1)$, $d_{\alpha N}(i, i + 2)$, $d_{\alpha N}(i, i + 3)$, and $d_{\alpha N}(i, i + 4)$ are labeled with both residue numbers. For Pro^{150}, the δ-CH2 signals substitute for the α-H signals. *B*, summary of the NOEs observed for the 19-residue wild type Ad5 peptide. The distance (Å) between the sequential ($(i, i + 1)$), medium ($(i, i + 2)$ and $(i, i + 3)$), and long range ($(i, i + 4)$) NOEs observed for the 19-residue Ad5 wild type CR3 peptide are represented by the *thickness* of the *bars*. NOEs of the type $(i, j + 2)$ $(i, j + 3)$, and $(i, j + 4)$ indicate classes other than $d_{\alpha N}$, d_{NN}, or $d_{\beta N}$. For Pro^{150}, the δ-CH_2 signals substitute for the α-H signals. Greater than 95% of prolines adopt a trans-peptide backbone conformation.

confirms that purified bacterially expressed Ad12 13 S E1A binds to TBP and that this interaction is not disrupted by washing with NETN buffer (*lane 1*). A similar interaction occurs between Ad12 12 S E1A and GST-TBP (Fig. 2*A*; *lane 2*), although it appears that considerably less Ad12 12 S E1A than 13 S E1A binds to TBP in this assay. Thus, determinants present in part of CR3 (*i.e.* the zinc finger) in the larger E1A molecule are important for the interaction. It should be noted that the monoclonal antibody 5D02 reacts somewhat more strongly with 13 S E1A than with 12 S E1A.[3]

Interactions of Ad E1A Peptides with TBP—In the absence of the full complement of structural determinants found in full-length E1A, the affinity of GST-TBP for the synthetic peptides is expected to be lower than for the intact protein. Thus, the ability of the synthetic peptides to disrupt Ad12 13 S E1A binding to GST-TBP was assessed under conditions where the peptide was present at a concentration far in excess of either GST-TBP or Ad12 13 S E1A.

The effect of increasing concentration of the 22-aa Ad12 peptide (amino acids 138–159; Fig. 1) upon the formation of the GST-TBP·Ad12 13 S E1A complex is shown in Fig. 2*B*. In the absence (Fig. 2*B*, *lane 1*) or presence of 3 nmol of peptide (Fig. 2*B*, *lane 3*) Ad12 13 S E1A was detected in the supernatant after elution with GST-TBP from the agarose with glutathione. However, in the presence of 12 nmol of peptide (excess of

[3] D. P. Molloy, K. J. Smith, A. E. Milner, P. H. Gallimore, and R. J. A. Grand, unpublished data.

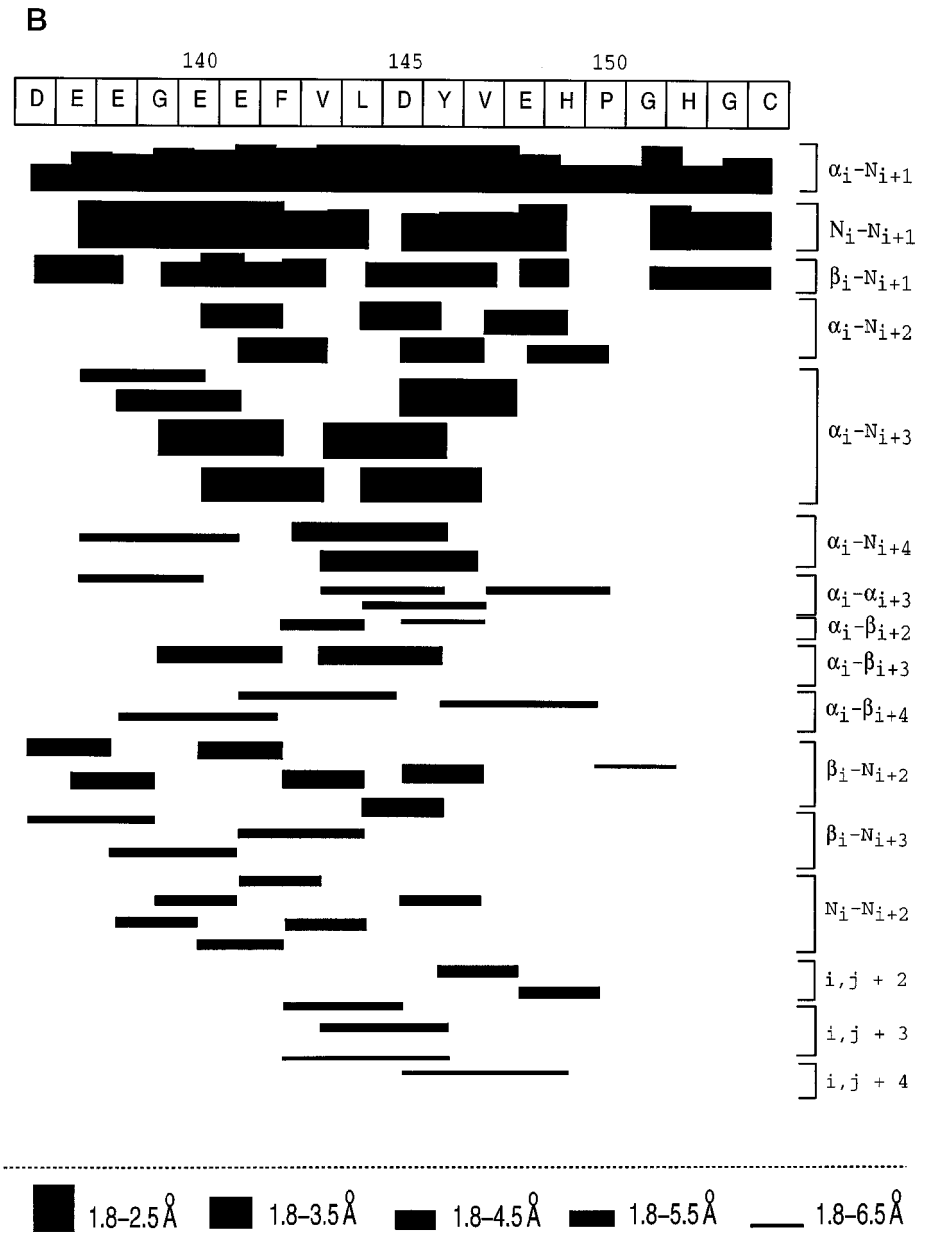

FIG.3—*continued*

peptide to E1A of 25:1), the GST-TBP·E1A complex was disrupted (Fig. 2*B*, *lane 2*), and therefore little E1A could be detected when TBP was displaced with glutathione. We have also examined the effect of peptides identical to the N terminus of CR3 from Ad5 13 S E1A upon the formation of GST-TBP·Ad12 13 S E1A complex. It was found that high concentrations of the wild type (Fig. 2*B*, *lane 4*) and mutant (V147L; Fig. 2*B*, *lane 6*) forms of the 19-residue Ad5 peptide (aa 136–154; Fig. 1.) disrupt the GST-TBP·E1A complex.

In addition, enzyme-linked immunosorbent assay techniques were employed (see "Experimental Procedures") to determine the affinity of GST-TBP for the various peptides, and the K_d values were evaluated. These were found to be 2.3×10^{-6}, 3.2×10^{-6}, and 2.1×10^{-6} M for the 19-aa wild type and V147L Ad5 CR3 peptides and the 22-aa Ad12 CR3 peptide, respectively (data not shown). In view of the dramatic competitive effects of the Ad5 and Ad12 peptides upon the interaction between Ad12 13 S E1A and GST-TBP, it was deemed essential to examine the structural properties of the peptides.

Structure of the 19-Residue Ad5 Wild Type CR3 Peptide—The structure of the 19-residue peptide identical to wild type Ad5 CR3 amino acids Asp^{136} to Cys^{154} (Fig. 1) was examined by ^{1}H NMR spectroscopy. A section from the NOESY spectrum (of mixing time 200-ms duration) of the peptide is shown in Fig. 3*A*, and a summary of the observed NOEs is illustrated in Fig. 3*B*. The calculated structure for the peptide is presented in Fig. 4. In the absence of long range NOE cross-peaks, the backbone conformation at the C terminus (residues Gly^{151}–Cys^{154}) of the peptide shows pronounced variation. Over residues Asp^{136}–Pro^{150}, the conformation of the peptide backbone is more ordered. On the basis of the types and relative volumes of the NOE cross-peaks $d_{\alpha N}(i, i + 3)$ NOEs Glu^{138}–Glu^{141}, Gly^{139}–Phe^{142}, Glu^{140}–Val^{143}, Val^{143}–Tyr^{146}, Leu^{144}–Val^{147}, Asp^{145}–Glu^{148} and $d_{\alpha N}(i, i + 4)$ NOEs Phe^{142}–Tyr^{146} and Val^{143}–Val^{147} (Fig. 3*B*), the region Asp^{136}–His^{149} forms a series of tight overlapping right-handed α-helical turns. Additionally, the side chain atoms of the residues involved in helix formation are unidirectional and adopt the classical α-helix side chain orientation. As expected, the peptide adopts a regular CO_i–$NH_{i, i+4}$ donor-acceptor α-helical hydrogen bonding pattern consistent with low temperature shift coefficients for Glu^{140} (1.9 ppb/K), Phe^{142} (3.0 ppb/K), Leu^{144} (2.0 ppb/K), and Tyr^{146} (2.5 ppb/K;

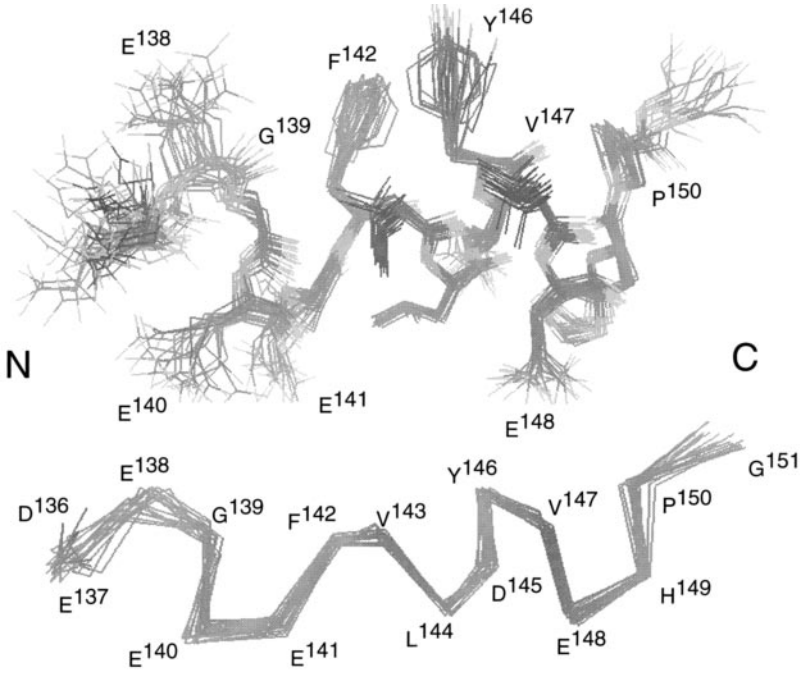

FIG. 4. **The calculated structure for the 19-residue wild type Ad5 peptide.** Twenty-one structures out of 100 calculated superimposed over the region Glu^{138}–Gly^{151} are shown. In the *upper panel*, both the backbone and side chain non-hydrogen atoms are illustrated. In the *lower panel*, only the α-carbon atoms are presented. Amino acids are labeled using the single letter abbreviation and number in the sequence of Ad5 13 S E1A. No distance restraint was violated by more than 0.3 Å.

data not shown).

The structure of a slightly shorter peptide, identical to amino acids Glu^{140}–Cys^{154} of the N terminus of CR3, was also examined. Once again, the peptide adopts a helical conformation in solution as defined by NOEs of the type $d_{\alpha N}(i, i + 2)$ Val^{143}–Asp^{145}, Leu^{144}–Tyr^{146}, Asp^{145}–Val^{147}, Tyr^{146}–Glu^{148} and $d_{\alpha N}(i, i + 3)$ Leu^{144}–Val^{147}, Val^{147}–Tyr^{146}, and Tyr^{146}–His^{149} (data not shown). In the shorter Ad5 CR3 peptide, the cooperative forces favoring α-helix formation are reduced, and the peptide tends toward a higher population of 3_{10}-helical turns.

Effect of Mutation on the Structure of the Ad5 Peptides—We assessed the structural consequences for the 19-residue Ad5 peptide of the conservative V147L mutation that has been proposed to have severe implications for the biological activity of the Ad5 13 S E1A protein (32). Apart from Tyr^{146} and Glu^{148}, which flank the mutation, the chemical shift positions of the backbone amide proton signals and NOEs observed within the mutant peptide were equivalent to those observed for the wild type form of the peptide (data not shown). It is possible to conclude on the basis of these data that the V147L peptide adopts a helical conformation that is not significantly different from the wild type form (Fig. 4). This finding is unusual in view of the dramatic effect of the V147L substitution upon the biological activity of Ad 5 E1A (32). Thus, further investigation of the structural properties of the 19-aa Ad5 wild type and mutant (V147L) CR3 peptides was deemed essential.

Secondary Structure of Ad5 CR3 Peptides Determined by CD Spectroscopy—To confirm similarities in secondary structure between the wild type and V147L forms of the 19-aa CR3 peptide, CD spectroscopy was performed (Fig. 5). It was found that the wild type Ad5 CR3 peptide adopts a stable helical conformation in solution (approximately 68%) as determined from the negative ellipsity at wavelengths between 220 and 230 nm (Fig. 5*A*). In addition, the helical conformation is unaffected by temperature. It was therefore of interest to observe that the mutant (V147L) form of the peptide also possesses helical propensity that is unaffected by temperature (Fig. 5*B*). On the basis of these results, there is little structural information that might explain the dramatic biological effects as a result of the V147L substitution (32).

Structure of the N Terminus of CR3 from Ad12 13 S E1A—Although conserved regions 2 and 3 from the nononcogenic Ad5 13 S E1A protein bear distinct sequence homology to the corresponding regions from the Ad12 protein, these regions are separated by 20 amino acids in Ad12 13 S E1A (Fig. 1). This spacer region has been shown, by mutational analysis, to be in part responsible for the oncogenic potential of the Ad12 13 S E1A protein (reviewed in Ref. 14). Therefore, it was of interest to examine the structural properties of a 22-aa peptide identical to residues Ala^{138}–Cys^{159} from Ad12 13 S E1A that spans the C-terminal seven residues of the oncogenic linker region and extends into the N terminus of CR3 (Fig. 1).

A summary of the NOEs observed for the 22-aa Ad12 CR3 peptide is shown in Fig. 6*A* along with the calculated structure in Fig. 6*B*. Inspection of the distribution of NOEs (Fig. 6*A*) reveals that few medium range cross-peaks were identified at the N terminus (aa Ala^{138}–Asp^{141}) and the C terminus (aa Glu^{153}–Cys^{159}). This results in a pronounced fraying of the backbone conformation over these regions (Fig. 6*B*). Once again there is a region of ordered helical structure in the backbone conformation, defined by medium and long range NOEs (summarized in Fig. 6*A*), that extends between residues Asp^{141} and His^{151} (Fig. 6*B*). However, the bulky side chains of Phe^{147}, Leu^{149}, and His^{151} are somewhat overcrowded compared with the classical α-helical conformation adopted by the Ad5 peptides (see above). Thus, amino acids between Asp^{141} and His^{151} in the Ad12 peptide form an irregular helix as a consequence of averaging over the conformational preferences on the NMR time scale.

Structural Implications for Ad12 CR3 on TBP Binding—To confirm the interaction of TBP with the Ad12 CR3 peptide (Fig. 2), TBP-induced structural changes within the peptide were examined in the presence of the increasing concentrations of TBP by one-dimensional NMR spectroscopy. Fig. 7 shows the downfield region of the one-dimensional spectrum for the 22-aa Ad12 CR3 peptide (Fig. 7*A*). When GST-TBP was added to the peptide, a number of specific changes were observed, which can be attributed to local structural changes resulting from TBP binding (Fig. 7*B*). Most notably, the signals of His^{151} and His^{157} C-4 protons are moved downfield, and the ring 3,5 signal of Phe^{147} experiences line-broadening effects (Fig. 7*B*). The labeled resonances probably represent an averaging of signals

due to fast exchange between the "bound" and "free" conformers of the peptide on the NMR time scale. Similar effects were observed in the one-dimensional spectra for the wild type and V147L forms of the 19-aa Ad5 CR3 peptide (data not shown). There was no discernable effect upon the peptide spectra in the presence of GST control protein (data not shown). It is possible to conclude on the basis of these data that residues C-terminal to the helix formed by residues Ala^{138}–His^{151} (*e.g.* His^{157}) also detect TBP binding.

DISCUSSION

Activation of a number of viral and cellular genes by Ad E1A can occur by CR3-dependent or CR3-independent mechanisms (reviewed in Ref. 34). Of particular importance to the activation properties of CR3 is this region's ability to bind TBP (27, 28), the DNA binding component of transcription factor IID. Deletion or mutation of the N-terminal segment of CR3 has been shown to disrupt the interactions of E1A with that protein (28, 31, 32). Additionally, mutations of amino acids that form part of the zinc finger motif located between residues 154 and 174 in Ad5 E1A (32) also disrupt the interaction between E1A and TBP.

Using short synthetic peptides, we have demonstrated that TBP will interact with an amino acid sequence present in both Ad5 and Ad12 13 S and 12 S E1A CR3 but that does not include any residues involved in the zinc finger (Fig. 2). We suggest that this region forms a major portion of the binding site *in vivo*. The binding of the smaller Ad12 E1A component to TBP has been confirmed by co-precipitation studies using purified proteins (Fig. 2). Whether the N-terminal region of E1A, recently shown to be involved in TBP binding (33), is partly responsible for this interaction is not clear at present and will have to await further investigation.

The three-dimensional structure of the CR3 peptides has been examined by two-dimensional ^{1}H NMR. TFE was used as a co-solvent with water in this study, since it is well known that TFE/water mixtures enhance the solution structures of small peptides, primarily by providing an environment in which hydrogen bond formation within the peptide is promoted. TFE also reduces the formation of spurious secondary structures as a result of hydrophobic aggregation (37, 44, 45). In the presence of trifluoroethanol, the observation of a helical conformation in small peptides that possess a high intrinsic helical capability is not uncommon (44, 45, 47). The data presented show that the N terminus of CR3 from Ad5 adopts a helical conformation in solution. Although a predominately 3_{10}-helical conformation was seen in the shorter Ad5 peptide, in the larger Ad5 peptide a regular α-helix is formed. The transition between random coil and α-helical conformations is believed to occur via a 3_{10}-helical intermediate in which the carbonyl oxygen acceptor in a CO_i–$NH_{i,\,i+3}$ hydrogen bond, forming an isolated turn, migrates to form a CO_i–$NH_{i,\,i+4}$ hydrogen bond (46). Therefore, it seems likely that the corresponding region in the parent protein will also prove to be a regular α-helix. As expected, the helical folding capability of the peptide increases as the peptide sequence length is increased. This situation was also found for the peptides that span the N terminus of CR3 from Ad12 E1A.

Previous mutational and biochemical analysis of E1A CR3 has focused upon the nononcogenic Ad5 serotype proteins (summarized in Ref. 32). Fig. 1 illustrates the sequence similarities between this region in Ad5 and the oncogenic Ad12 13 S E1A, and this suggests that similar structures might exist in the two proteins. It can be seen that the helices that have been determined (Figs. 5 and 6) comprise slightly different amino acids in Ad5 and Ad12. The 22-residue Ad12 peptide described in this work contains the C-terminal portion of the oncogenic spacer (AAADRER) and therefore extends slightly further toward the N terminus of the protein than is the case for the 19-residue Ad5 CR3 peptide. Thus, while the structural motif is conserved between the virus serotypes, its precise position is not. However, this is unlikely to be a direct consequence of the particular extra residues present and more probably is simply a result of increased peptide length used in this study. Despite this, the presence of the oncogenic spacer directly N-terminal to CR3 may have important structural and biological consequences in the intact Ad12 E1A. This is particularly relevant, since the spacer region contains a predominance of alanine residues. It is well documented that alanine-rich peptides adopt a helical conformation in solution (47). The presence of such a local configuration has been proposed to function as a polypeptide spacer region (48). Thus, it is possible that the helix seen in the N terminus of CR3 could extend through the oncogenic spacer region in Ad12 E1A. Such a prominent structural motif could be important for the interactions with TBP or with other E1A-binding proteins responsible for the oncogenic potential of Ad12 E1A (14).

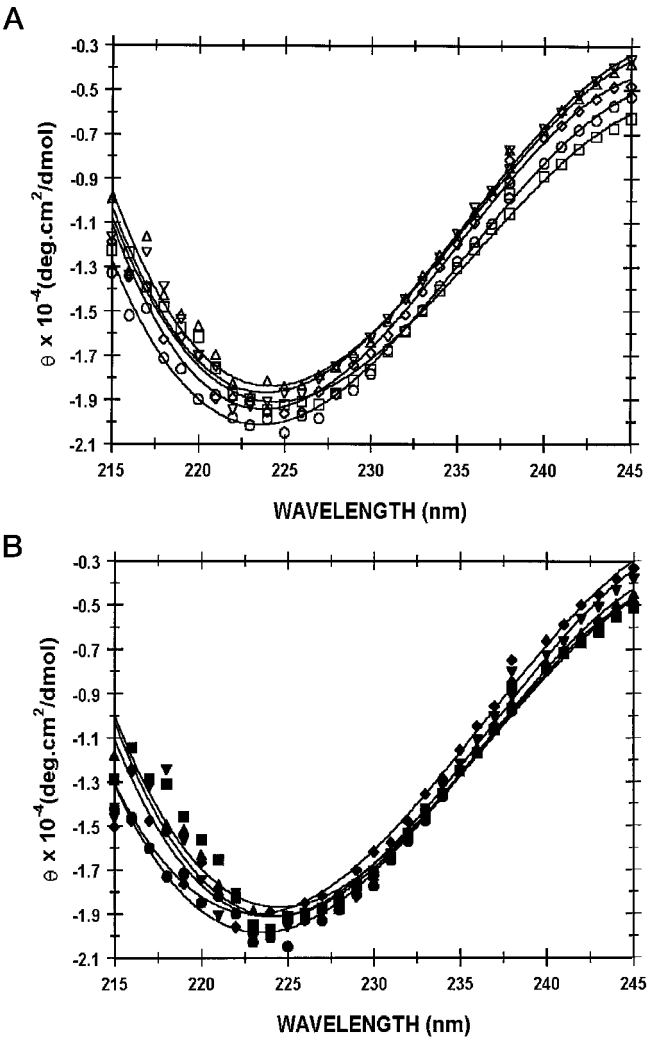

FIG. 5. **Far UV circular dichroism spectra of Ad E1A CR3 peptides.** The circular dichroism spectra of the wild type (*A*) and the V147L mutant (*B*) forms of the 19-aa Ad5 CR3 peptide recorded in 1 mM Tris·HCl, pH 7.4, are illustrated. Spectra were recorded at the temperatures of 25 °C (□, wild type; ■, mutant), 35 °C (○, wild type; ●, mutant), 45 °C (△, wild type; ▲, mutant), 55 °C (▽, wild type; ▲, mutant), and 65 °C (◇, wild type; ◆, mutant). Peptide concentrations were 100 μM. Each spectrum represents the average from five experiments. The *solid lines* represent best fit of the data by a polynomial regression function accounting for at least 68% of peptide residues adopting α-helical turns between 220 and 230 nm.

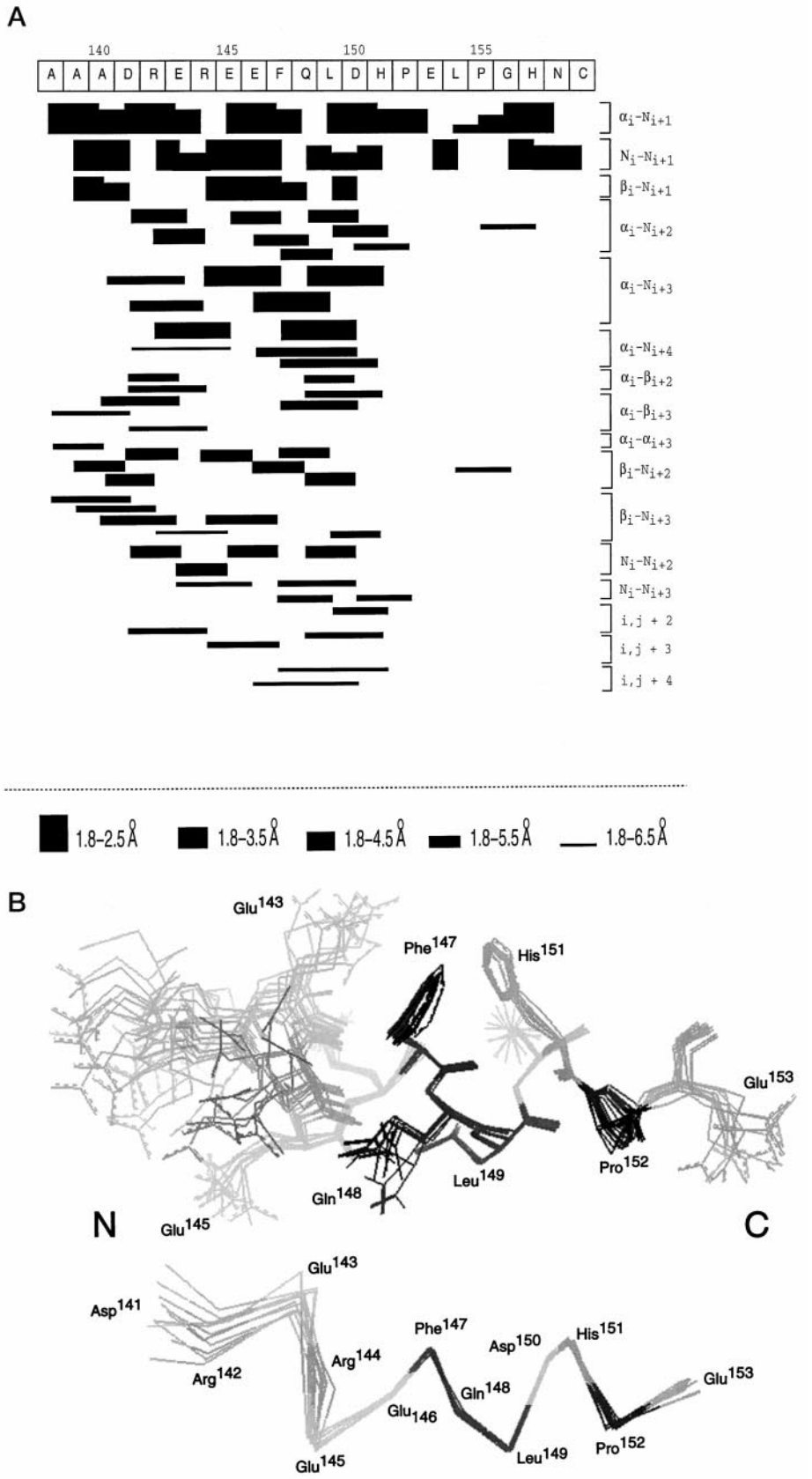

FIG. 6. **Structural properties of the 22-residue Ad12 (aa 138–159) synthetic peptide.** *A*, summary of the sequential, medium, and long range signals. The distance (Å) of the sequential ((i, i + 1)), medium ((i, i + 2) and (i, i + 3)), and long range (i, i + 4) NOEs observed for the 22-residue Ad12 CR3 peptide of sequence AAADREREEFQLDVPELPGHNC in 50% (v/v) TFE at 285 K are represented by the *thickness* of the *bars*. Cross-peaks defined as (i,j + 2) and (i,j + 3) indicate classes other than $d_{\alpha N}$, d_{NN}, or $d_{\beta N}$ types. For Pro^{152} and Pro^{155} the δ-CH2 signals substitute for the α-H signals. Greater than 95% of prolines adopt a trans-peptide backbone conformation. *B*, the calculated structure for the 22-residue Ad12 peptide. Ten structures out of 75 calculated superimposed over the region Asp^{141}–Glu^{153} are illustrated. The *top* shows the backbone and side chain non-hydrogen atoms. In the *bottom* only the α-carbon atoms are presented. Amino acids are labeled using the three-letter abbreviation and number in the sequence of Ad12 13 S E1A. No distance restraint was violated by more than 0.5 Å.

The helical conformation formed by residues within the N terminus of both Ad5 and Ad12 CR3 is likely to play an essential part in mediating the interaction between E1A and TBP, and information concerning this can be gained from NMR studies on the bound form of the peptides. In addition, it appears from the data presented in Fig. 7 that residues C-terminal to the α-helical region could be involved in binding to TBP, with observed perturbations of signals attributable to His^{151}, His^{157}, and Phe^{147}.

Interestingly, it has recently been shown, by mutational

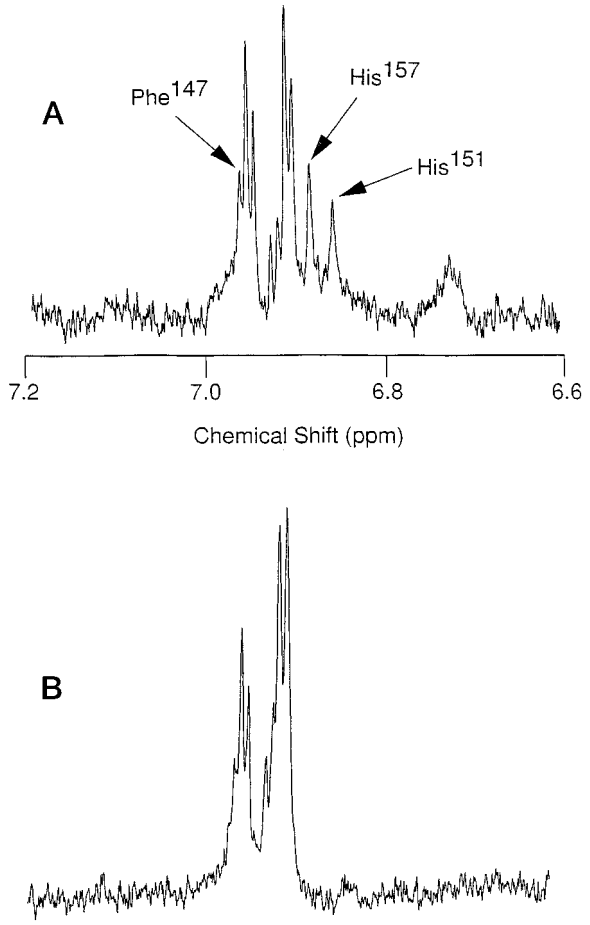

FIG. 7. **One-dimensional ^{1}H NMR analysis of Ad12 22-aa peptide interactions with GST-TBP.** The aromatic region of the one-dimensional spectra recorded on a 300 μM sample of the 22-aa Ad12 CR3 peptide at 293 K in 25 mM [^{2}H]Tris, adjusted to pH 7.4 with ^{2}HCl in the absence (*A*) and in the presence (*B*) of 15 μM GST-TBP, are presented. Assignments for the C4-H signals of His^{149}, His^{157}, and the 3,5H ring proton of Phe^{147} (labeled using the sequence of Ad12 266-aa E1A) were determined from a two-dimensional TOCSY experiment performed on the Ad12 CR3 peptide in 25 mM [^{2}H]Tris, adjusted to pH 7.4 with ^{2}HCl at 293 K in the absence of GST-TBP. Spectra are presented after subtraction of protein background.

analyses, that charged residues on the surface helix, H2, of TBP form an essential portion of the interface upon formation of the TBP·TFIIA (49) and TBP·Brf (50) complexes. It is possible that the complex formed between E1A and TBP could be, in part, mediated through helices in both CR3 and the basic region between residues 221–271 in TBP. However, mutational analysis has shown that acidic amino acids at the extreme N terminus of CR3 are not solely responsible for binding to TBP (28).

In these structural studies, we have attempted to examine the consequences of biologically significant mutations. We have demonstrated that there is little or no significant difference between wild type and V147L mutant forms of the Ad5 19-residue peptide in their affinity for TBP, CD spectra, and calculated structures. These findings are of particular interest, since a published report suggests that the Ad5 13 S E1A protein carrying the V147L substitution (32) does not interact with TBP. Therefore, the inhibitory activity displayed by the V147L mutant protein (32) could in principle be achieved by one of two mechanisms. First, the substitution could alter the local backbone configuration of E1A and disrupt the three-dimensional orientation of the proteins in the wild type E1A·TBP complex. Second, the substitution could disrupt the hydrophobic bonding pattern or induce a steric constraint upon formation of the E1A·TBP complex.

Our data suggest that the backbone folding pattern is unaffected by the V147L substitution. Additionally, the ability of the V147L peptide to inhibit the binding of E1A to TBP argues against any hydrophobic or steric effects. Thus, we can offer no structural explanation to account for the findings of Geisberg *et al.* (32). However, it is possible that substitution of Val^{147} with Leu may have long range tertiary structural repercussions for the protein that would not be seen in the experiments described here. It has also been noted that the E148G and P150G substitutions reduce the interaction of E1A with TBP (28, 32). It is probable that the presence of a glycine residue would disrupt the helix observed in the Ad5 synthetic peptides described here and in the TBP binding site *in vivo*. We attempted to analyze the effect of the P150G mutation (32) but found that an equivalently substituted 15-aa peptide (equivalent to Ad5 CR3) aggregated in solution. We suggest that the change in properties of the P150G peptide is indicative of profound changes occurring in the structure of this part of the intact protein as a result of the mutation.

In summary, we have shown that relatively short synthetic peptides equivalent to parts of Ad5 and Ad12 E1A conserved region 3 are highly ordered structures in solution. The three-dimensional conformations observed are consistent with α-helices, which, we suggest, are likely to be similar to the structures present in these regions of the intact proteins. The helices extend minimally from Ala^{139} to His^{151} in Ad12 and from Glu^{140} to Glu^{148} in Ad5 and probably comprise at least an important part of the binding site for TBP. It is interesting to note that the V147L mutation that reduces TBP binding and trans-activation in Ad5 has only very subtle structural repercussions in this region. It is suggested that this amino acid could participate in long range structural determinants.

Acknowledgments—We are most grateful to the Wellcome Trust and the University of Birmingham Biological NMR Unit for the provision of facilities and to A. J. Pemberton for maintaining these facilities. We thank Dr. M. Mezna (University of Birmingham) for performing the CD experiments and Professor I. P. Trayer for helpful discussions of this work.

REFERENCES

1. Jones, N., and Shenk, T. (1979) *Proc. Natl. Acad. Sci. U. S. A.* **76,** 3656–3669
2. Berk, A. J., Lee, F., Harrison, T., Williams, J., and Sharp, P. A. (1979) *Cell* **17,** 935–944
3. Boulanger, P. A., and Blair, G. E. (1991) *Biochem. J.* **275,** 281–299
4. Shenk, T., and Flint, J. (1991) *Adv. Cancer Res.* **57,** 47–85
5. Rao, L., Debbas, M., Sabbatini, P., Hockenberry, D., Kormeyer, S., and White, E. (1992) *Proc. Natl. Acad. Sci. U. S. A.* **89,** 7742–7746
6. Debbas, M., and White, E. (1993) *Genes Dev.* **7,** 546–554
7. Braithwaite, A. W., Cheetham, B. F., Li, P., Parish, C. R., Waldron-Stevens, L. K., and Bellet, A. J. D. (1983) *J. Virol.* **45,** 192–199
8. Quinlan, M. P., and Grodzicker, T. (1987) *J. Virol.* **61,** 673–682
9. Webster, K. A., Muscat, G. E. O., and Kedes, L. (1988) *Nature* **332,** 553–557
10. Kalman, D., Whittaker, K., Bishop, J. M., and O'Lague, P. H. (1993) Mol. Biol. Cell **4,** 353–361
11. Gallimore, P. H., Byrd, P. J., Whittaker, J. L., and Grand, R. J. A. (1988) Cancer Res. **45,** 2670–2680
12. Moran, E. (1994) *Semin. Virol.* **5,** 327–340
13. Bayley, S. T., and Mymryk, J. S. (1995) *Int. J. Oncol.* **5,** 425–444
14. Williams, J., Williams, M., Lu, C., and Telling, G. (1994) *Curr. Topics Microbiol. Immunol.* **199,** 149–175
15. Whyte, P., Williamson, N. M., and Harlow, E. (1989) *Cell* **56,** 67–75
16. Dyson, N., Guida, P., McCall, C., and Harlow, E. (1992) *J. Virol.* **66,** 4606–4611
17. Wang, H-G. H., Rikitake, Y., Carter, M. C., Yaciuk, P., Abraham, S. E., Zerler, B., and Moran, E. (1993) *J. Virol.* **67,** 476–488
18. Eckner, R., Ewen, M. E., Newsome, D., Gerdes, M., Deaprio, A., Lawrence, J. B., and Livingston, D. M. (1994) *Genes Dev.* **8,** 869–884
19. Kimelman, D., Miller, J. S., Porter, D., and Roberts, B. E. (1985) *J. Virol.* **53,** 399–409
20. Moran, E., and Mathews, M. (1987) *Cell* **48,** 177–178
21. Boyd, J. M., Subramanian, T., Schaefer, U., La Regina, M., Bayley, S., and Chinnadurai, G. (1993) *EMBO J.* **12,** 469–478
22. Pei, R., and Berk, A. J. (1989) *J. Virol.* **63,** 3499–3506
23. Lui, F., and Green, M. R. (1990) *Cell* **61,** 1217–1224
24. Lui, F., and Green, M. R. (1994) *Nature* **368,** 520–525

25. Chatton, B., Bocco, J., Gaire, M., Hauss, C., Reimund, B., Goetz, J., and Kedinger, C. (1993) *Mol. Cell. Biol.* **13,** 561–570
26. Lewis, B. A., Tullis, G., Seto, E., Horkoshi, N., Weinmann, R., and Shenk, T. (1995) *J. Virol.* **69,** 1628–1636
27. Horkoshi, N., Maguire, K. J., Kralli, A., Maldonado, E., Reinberg, D., and Weinmann, R. (1991) *Proc. Natl. Acad. Sci. U. S. A.* **88,** 5124–5128
28. Lee, W. S., Kao, C., Bryant, G. O., Liu, X., and Berk, A. J. (1991) *Cell* **67**, 365–376
29. Culp, J. S., Webster, L. C., Friedman, D. J., Smith, C. L., Huang, W-J., Wu, F. Y-H., Rosenberg, M., and Ricciardi, R. P. (1988) *Proc. Natl. Acad. Sci. U. S. A.* **85,** 6450–6454
30. Webster, L. C., Zhang, K., Chance, B., Ayene, I., Culp, J. S., Huang, W-J., Wu, F. Y.-H., and Ricciardi, R. P. (1991) *Proc. Natl. Acad. Sci. U. S. A.* **88,** 9989–9993
31. Webster, L. C., and Ricciardi, R. P. (1991) *Mol. Cell. Biol.* **11,** 4287–4296
32. Geisberg, J. V., Lee, W. S., Berk, A. J., and Ricciardi, R. P. (1994*) Proc. Natl. Acad. Sci. U. S. A.* **91,** 2488–2492
33. Lipinski, K. S., Esche, H., and Brockmann, D. (1997) *Virus Res.* **54,** 99–106
34. Jones, N. (1995) *Curr. Topics Microbiol. Immunol.* **199,** 59–80
35. Segawa, S.-I., Fukuno, T., Fujiwara, K., and Noda, Y. (1991) *Biopolymers* **31**, 497–509
36. Smith, L. J., Alexandrescu, A. T., Pitkeathly, M., and Doson, C. M. (1994) *Structure* **2,** 703–712
37. Molloy, D. P., Milner, A. E., Yakub, I. K., Chinnadurai, G., Gallimore, P. H., and Grand, R. J. A. (1998) *J. Biol. Chem.* **273,** 20867–20876
38. Lillie, J. W., Loewenstein, P. M., Green, M. R., and Green, M. (1987) *Cell* **50**, 1091–1100
39. Grand, R. J. A., Gash, L., Milner, A. E., Molloy, D. P., Turnell, A. T., Szestak, T., and Gallimore, P. H. (1998) *Virology* **244,** 230–242
40. Grand, R. J. A., and Gallimore, P. H. (1984) *J. Gen. Virol.* **65,** 2149–2166
41. Piotto, M., Saudek, V., and Skelnar, V. (1992) *J. Biomol. NMR* **2,** 661–665
42. Kay, L. E., Keifer, P., and Saarinen, T. (1994) *J. Magn. Reson. Ser. B* **103**, 203–216
43. Brünger, A. T. (1992) *X-PLOR, version 3.1: A System for X-ray Crystallography* and NMR, Yale University Press, Cambridge, MA
44. Smith, K. J., Trayer, I. P., and Grand, R. J. A. (1994) *Biochemistry* **33,** 6063–6073
45. Smith, K. J., Scotland, G., Beattie, J., Trayer, I. P., and Houslay, M. D. (1996) J. Biol. Chem. **271,** 16703–16711
46. Tirado-Rives, J., and Jørgenson, W. L. (1991) *Biochemistry* **30,** 3864–3871
47. Miick, S. M., Martinez, G. V., Fiori, W. R., Todd, A. P., and Millhauser, G. L. (1992) *Nature* **359,** 653–655
48. Crisma, M., Valle, G., Moretto, V., Formaggio, F., and Toniolo, C. (1995) *Peptide Res.* **8,** 187–190
49. Bryant, G. O., Martel, L. S., Burley, S. K., and Berk, A. J. (1996) *Genes Dev.* **10,** 2491–2504
50. Shen, Y., Kassavetis, G. A., Bryant, G. O., and Berk, A. J. (1998) *Mol. Cell. Biol.* **18,** 1692–1700